


Effects of Nonlinear Damping on Vibrations of Microbeam

Kun Huang^{1,2,*} , Tianpeng Li¹, Wei Xu¹ and Liang Cao¹

¹ Department of Engineering Mechanics, Faculty of Civil Engineering and Mechanics, Kunming University of Science and Technology, Kunming 650500, China; litianpeng528@163.com (T.L.); 13354909706@163.com (W.X.); caoliang1106@126.com (L.C.)

² Yunnan Key Laboratory of Disaster Reduction in Civil Engineering, Kunming University of Science and Technology, Kunming 650500, China

* Correspondence: kunhuang@kust.edu.cn; Tel.: +86-158-7795-2802

Abstract: The present paper develops a new Bernoulli–Euler theory of microbeams for the consideration of small-scale effects and nonlinear terms, which are induced by the axial elongation of the beam and Kelvin–Voigt damping. The non-resonance and primary resonance of microbeams are researched through the application of Galerkin and multiple scale methods to the new model. The results suggest the following: (1) Nonlinear damping slightly affects the vibration amplitudes under the non-resonance condition; (2) nonlinear damping can significantly change the bifurcation points that induce a jump in the vibration amplitudes under the primary resonance condition. The current researches indicate that nonlinear damping is necessary for an accurate description of microbeam vibrations.

Keywords: Bernoulli–Euler microbeam; modified couple stress theory; nonlinear vibrations; damping; multiple scale method



Citation: Huang, K.; Li, T.; Xu, W.; Cao, L. Effects of Nonlinear Damping on Vibrations of Microbeam. *Appl. Sci.* **2022**, *12*, 3206. <https://doi.org/10.3390/app12063206>

Academic Editor: César M. A. Vasques

Received: 9 February 2022

Accepted: 10 March 2022

Published: 21 March 2022

Publisher's Note: MDPI stays neutral with regard to jurisdictional claims in published maps and institutional affiliations.



Copyright: © 2022 by the authors. Licensee MDPI, Basel, Switzerland. This article is an open access article distributed under the terms and conditions of the Creative Commons Attribution (CC BY) license (<https://creativecommons.org/licenses/by/4.0/>).

1. Introduction

A study of the dynamics and energy dissipation of microbeams is necessary, since slender beams are frequently used in micro-scale devices and systems, such as microelectromechanical systems (MEMS) [1–3].

A crucial issue of the mechanical properties of microbeams is the size-independent behavior observed in micro-scale experiments [4–6]. McFarland and Colton observed that the microbeam's flexural rigidity is at least four times larger than the one predicted by the classical beam theory [4]. Fleck found that the dimensionless torque increases the classical torque theory by three times when the wire diameter decreases from 170 to 12 μm [5]. Stölken and Evans found that the dimensionless flexural rigidity increases significantly as the beam thickness decreases from 50 to 12.5 μm [6]. However, the classical slender beam models based on the classical elasticity cannot describe this size effect due to the lack of material length scale parameters. This disadvantage motivated the development of beam theories using nonlocal elasticity theories to model nanobeams [7,8] and higher-order strain gradient theories to model microbeams [3,9–11]. Moreover, almost all of the existing microbeam models are based on linear constitutive relations. However, the material nonlinearity also influences the mechanical properties of nanobeams [12].

The modified couple stress theory is widely accepted to model the mechanical properties of microbeams [13]. The couple stress tensor is symmetric and only involves one internal material length scale parameter in the modified couple stress theory. Based on this theory, the linear and nonlinear Bernoulli–Euler and Timoshenko microbeam models have been proposed [14–20]. Nevertheless, most of the studies on microbeam vibrations have overlooked the nonlinear terms, which are induced by damping. For example, the authors of [3,11,19] only considered the linear term of damping, while the authors of [11,16] completely overlooked it. The energy dissipation is related to the vibration frequencies

of the structures [21]. In macrostructures, nonlinear damping is almost smaller than the geometrical nonlinear, which is induced by the finite deformations [22]. However, since the vibration frequencies of microbeams are significantly higher than the macrobeams, nonlinear damping significantly affects the microstructure vibrations. Based on the modified couple stress theory, the present paper will propose a new Bernoulli–Euler model that includes the small-size effect and nonlinear terms, which are induced by the axial elongation of the beam and Kelvin–Voigt damping. Then, the effects of nonlinear damping are studied for the non-resonance and primary resonance.

2. Methods

In the modified couple stress theory, the symmetric couple stress characterizes the small-scale effect, and the strain energy density can be written as [13,23]:

$$U = \frac{1}{2}(\sigma_{ij}\epsilon_{ij} + m_{ij}\chi_{ij}), \quad (i, j = x, y, z) \tag{1}$$

where ϵ_{ij} and σ_{ij} are the stress and strain, $m_{ij} = 2G\zeta^2\chi_{ij}$ is the couple stress tensor, $\chi_{ij} = \frac{1}{2}[\nabla\omega + (\nabla\omega)^T]$ is the symmetrical curvature tensor, $\omega = (\nabla \times u)/2$ with u being the displacement vector [13], and $G = E/[2(1 + \nu)]$. Here, E and ν are the Young’s modulus and Poisson’s ratio, ζ is the material length scale parameter obtained from the experimentations. Based on the modified couple stress theory, Xia established an integral differential equation to model the mechanical properties of microbeams, as shown in Figure 1. This theory takes into account the small-scale effect and nonlinear damping, which are induced by the elongation of the microbeam [16]:

$$m \frac{\partial^2 w}{\partial t^2} + (EI + GS\zeta^2) \frac{\partial^4 w}{\partial x^4} + \left[P_0 - \frac{ES}{2L} \int_0^L \left(\frac{\partial w}{\partial x} \right)^2 dx \right] \frac{\partial^2 w}{\partial x^2} = F(x, t) \tag{2}$$

where w is the vertical deflection, P_0 and m are the initial axial load and mass per unit length, respectively, S and I are the cross-sectional area and moment of inertia. From Equation (2), it is found that the small-scale effect significantly affects the static bending and vibration frequencies of microbeams [16]. However, Equation (2) is an integral differential equation, and it is not easy to find solutions to the equation. As shown below, we will develop a new differential equation to replace Equation (2).

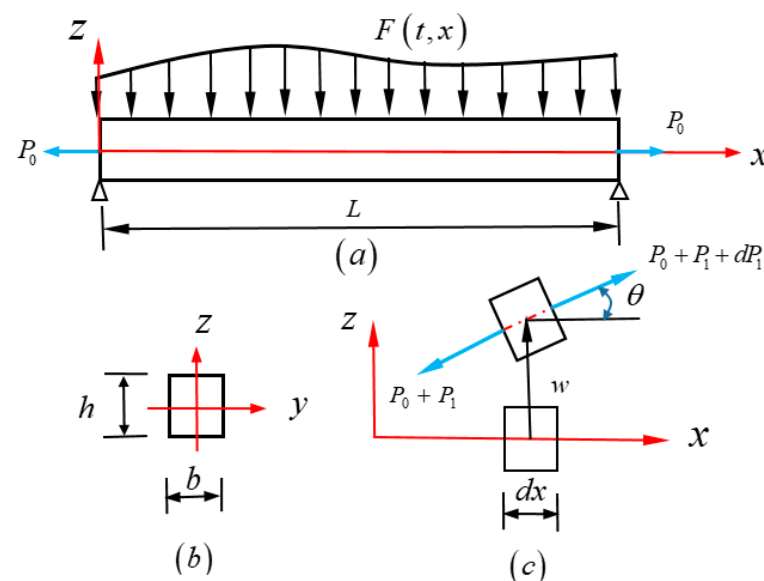


Figure 1. Portrait of the structure: (a) The undeformed coordinate system, (b) cross-section, (c) the displacement and rotation angle.

Suppose that the average axial force, which is induced by the axial elongation of the beam, is \bar{P}_1 , thus we obtain:

$$\bar{P}_1 = \frac{ES(\tilde{L} - L)}{L} \approx \frac{ES}{2L} \int_0^L (\partial w / \partial x)^2 dx \tag{3}$$

where $\tilde{L} = \int_0^L [1 + (\partial w / \partial x)^2 / 2] dx$ is the deformed length of the beam axle. On the beam element, the z component of the axial force increment is $(dP_1) \cdot \sin \theta$, and θ is the rotation angle of the cross-section, as shown in Figure 1c. Considering $\bar{P}_1 \approx P_1$, $\sin \theta \approx \theta$, $\theta \approx \partial w / \partial x$, and using Equation (3), we obtain:

$$\frac{\partial}{\partial x} (P_1 \sin \theta) dx \approx \frac{\partial}{\partial x} \left(\bar{P}_1 \frac{\partial w}{\partial x} \right) dx \approx \frac{ES}{2L} \left\{ \left[\frac{\partial^2 w}{\partial x^2} \int_0^L \left(\frac{\partial w}{\partial x} \right)^2 dx \right] \right\} dx \tag{4}$$

The right part of Equation (4) is also the nonlinear term of Equation (2). Equation (3) indicates that the accurate axial force P_1 is replaced by the average axial force \bar{P}_1 in Equation (2). The accurate force, which is induced by the axial elongation, can be written as $P_1 = ES(\Delta L / dx) \approx (ES/2)(\partial w / \partial x)^2$, where ΔL is the elongation of the element. Considering $d(P_1 \sin \theta) \approx (3ES/2)(\partial w / \partial x)^2 (\partial^2 w / \partial x^2) dx$, and Equation (4), we obtain:

$$\left[\frac{ES}{2L} \int_0^L \left(\frac{\partial w}{\partial x} \right)^2 dx \right] \frac{\partial^2 w}{\partial x^2} \approx \frac{3ES}{2} \left(\frac{\partial w}{\partial x} \right)^2 \frac{\partial^2 w}{\partial x^2} \tag{5}$$

Equation (5) indicates that the nonlinear differential term can replace the nonlinear term of Equation (2). Furthermore, Equation (2) does not consider the structural damping. Here, we suppose that Kelvin–Voigt damping is in the beams, thus E in Equation (2) will be replaced by $E + \tilde{E} \partial / \partial t$ [21,24], where \tilde{E} is the viscous damping coefficient. Substituting Equation (5) into Equation (2), the nonlinear equation, which includes the small-scale effect and nonlinear damping term, can be obtained as:

$$m \frac{\partial^2 w}{\partial t^2} + \tilde{E} \frac{\partial}{\partial t} \left[I \frac{\partial^4 w}{\partial x^4} - \frac{3S}{2} \left(\frac{\partial w}{\partial x} \right)^2 \frac{\partial^2 w}{\partial x^2} \right] + P_0 \frac{\partial^2 w}{\partial x^2} + (EI + GS\zeta^2) \frac{\partial^4 w}{\partial x^4} - \frac{3ES}{2} \left(\frac{\partial w}{\partial x} \right)^2 \frac{\partial^2 w}{\partial x^2} = F \tag{6}$$

Kahrobaian et al. studied the primary resonance, super-resonance, and sub-resonance of microbeams using Equation (2) with linear damping $\tilde{E} \partial w / \partial t$ [11]. In the present paper, we will focus on the effects of nonlinear damping. Let $\tilde{x} = x / L$, $\tilde{w} = w / L$, $\tilde{t} = \omega_0 t$ normalize the variables in Equation (6), thus we obtain:

$$\frac{\partial^2 \tilde{w}}{\partial \tilde{t}^2} + \pi^{-4} \frac{\partial^4 \tilde{w}}{\partial \tilde{x}^4} + P \frac{\partial^2 \tilde{w}}{\partial \tilde{x}^2} + C_1 \frac{\partial^5 \tilde{w}}{\partial \tilde{t} \partial \tilde{x}^4} - D \left(\frac{\partial \tilde{w}}{\partial \tilde{x}} \right)^2 \frac{\partial^2 \tilde{w}}{\partial \tilde{x}^2} - C_2 \frac{\partial}{\partial \tilde{t}} \left[\left(\frac{\partial \tilde{w}}{\partial \tilde{x}} \right)^2 \frac{\partial^2 \tilde{w}}{\partial \tilde{x}^2} \right] = \tilde{f} \tag{7}$$

The parameters in Equation (7) can be written as:

$$P = \frac{P_0}{mL^2\omega_0^2}, C_1 = \frac{\tilde{E}I}{mL^4\omega_0}, C_2 = \frac{3\tilde{E}S}{2mL^2\omega_0}, D = \frac{3ES}{2mL^2\omega_0^2}, \tilde{f} = \frac{F}{Lm\omega_0^2} \tag{8}$$

where $\omega_0 = \sqrt{\pi^4(EI + GS\zeta^2)(mL^4)^{-1}}$ is the natural frequency of the microbeam. For the same I / L^4 , the microbeam’s natural frequency ω_0 is more than the macrobeam, since the macrobeam’s mass per unit length is less than the microbeam. Therefore, the nonlinear

damping term of the microbeam is larger than the correspondent term of the macrobeam due to $D/C_2 = E/(\tilde{E}\omega_0)$. The boundary conditions for hinged–hinged microbeams can be written as:

$$\bar{w}(0, \bar{t}) = \bar{w}(1, \bar{t}) = 0, \quad \frac{\partial^2 \bar{w}}{\partial \bar{x}^2}(0, \bar{t}) = \frac{\partial^2 \bar{w}}{\partial \bar{x}^2}(1, \bar{t}) = 0 \tag{9}$$

Moreover, it is not easy to obtain an accurate analytical solution, since Equation (7) is the nonlinear differential equation. Therefore, we will use the Galerkin method to obtain an approximate analytical solution [24–26]. Suppose that the solution of Equation (7) can be written as:

$$\bar{w} = \sum_{j=1}^{\infty} \sin(j\pi\bar{x}) \eta_j(\bar{t}) \tag{10}$$

Substituting Equation (10) into Equation (7), then multiplying $\sin \pi\bar{x}$ by both sides of the equations, and integrating it in $[0, 1]$, the first-mode truncation of Galerkin method [24], which is an ordinary differential equation in time, can be obtained as:

$$\ddot{\eta} + 2\tilde{c}_1\dot{\eta} + \omega^2\eta + d\eta^3 + c_2\dot{\eta}\eta^2 = f(\bar{t}). \tag{11}$$

Here, we let $\eta = \eta_1$ and $\omega^2 = 1 - N\pi^2$, $\tilde{c}_1 = \pi^4 C_1/2$, $d = \pi^4 D/4$, $c_2 = 3\pi^4 C_2/4$.

3. Results

In this section, the multiple scale method [24–26], which is widely used to solve weak nonlinear differential equations [27–30], will be applied to Equation (11). Let $\tilde{c}_1 = \varepsilon^2 c_1$, $f(t) = \varepsilon f_1 \cos(\Omega_1 t) + \varepsilon^3 f_1 \cos(\Omega_2 t)$, then we obtain:

$$\ddot{\eta} + \omega^2\eta + \varepsilon^2 c_1\dot{\eta} + d\eta^3 + c_2\dot{\eta}\eta^2 = \varepsilon f_1 \cos(\Omega_1 t) + \varepsilon^3 f_2 \cos(\Omega_2 t) \tag{12}$$

Suppose

$$\eta(t; \varepsilon) = \varepsilon \eta_1(T_0, T_2) + \varepsilon^3 \eta_3(T_0, T_2) \tag{13}$$

where $T_0 = \bar{t}$ and $T_2 = \varepsilon^2 \bar{t}$. Substituting Equation (13) into Equation (12), then equating the coefficients of ε and ε^3 on both sides, we obtain:

$$\varepsilon : \frac{\partial^2 \eta_1}{\partial T_0^2} + \omega^2 \eta_1 = \frac{1}{2} f_1 \exp(i\Omega_1 T_0) \tag{14}$$

$$\begin{aligned} \varepsilon^3 : \frac{\partial^2 \eta_3}{\partial T_0^2} + \omega^2 \eta_3 &= -2 \frac{\partial}{\partial T_0} \left(\frac{\partial \eta_1}{\partial T_2} \right) \\ -2c_1 \frac{\partial \eta_1}{\partial T_0} - d\eta_1^3 - c_2 \eta_1^2 \frac{\partial \eta_1}{\partial T_0} + \frac{1}{2} f_2 \exp(i\Omega_2 T_0) \end{aligned} \tag{15}$$

The solution of Equation (14) can be written as:

$$\eta_1 = A(T_2) \exp(i\omega T_0) + \Lambda \exp(i\Omega_1 T_0) + cc \tag{16}$$

where $\Lambda = \frac{1}{2} f_1 (\omega^2 - \Omega_1^2)^{-1}$. Substituting Equation (16) into Equation (15), we obtain:

$$\begin{aligned} \frac{\partial^2 \eta_3}{\partial T_0^2} + \omega^2 \eta_3 &= \frac{1}{2} f_2 \exp(i\Omega_2 T_0) - [i2\omega(A' + c_1 A) \\ &+ (i2c_2\omega + 6d)\Lambda^2 A + (ic_2\omega + 3d)A^2 \bar{A}] \exp(i\omega T_0) + NST \end{aligned} \tag{17}$$

where NST denotes non-secular terms [26], and the prime indicates differentiation with respect to T_2 for simplicity.

3.1. Non-Resonant Hard Excitation

When the frequency of the load Ω_1 is further than the modal frequency ω , the condition for eliminating secular terms of Equation (17) can be written as:

$$i2\omega(A' + c_1A) + (i2c_2\omega + 6d)\Lambda^2A + (ic_2\omega + 3d)A^2\bar{A} = 0 \tag{18}$$

Suppose

$$A = \frac{1}{2}\alpha \exp(i\beta) \tag{19}$$

where α and β are real. Substituting Equation (19) into Equation (18), and separating the real and imaginary parts, we obtain:

$$\alpha' = \left(-c_1 - c_2\Lambda^2\right)\alpha - \frac{1}{8}c_2\alpha^3, \quad \alpha\beta' = \frac{3d}{\omega}\left(\Lambda^2 + \frac{1}{8}\alpha^2\right)\alpha \tag{20}$$

For steady-state solutions of Equation (20), we obtain $\alpha' = \beta' = 0$. Therefore, α and β are the solutions of

$$\left(-c_1 - c_2\Lambda^2\right)\alpha - \frac{1}{8}c_2\alpha^3 = 0, \quad \frac{3d}{\omega}\left(\Lambda^2 + \frac{1}{8}\alpha^2\right)\alpha = 0 \tag{21}$$

The first-order approximate solution of the non-resonant hard excitation can be written as:

$$\eta = \varepsilon[\alpha \cos(\omega T_0 + \beta) + \Lambda \cos(\Omega_1 T_0)] \tag{22}$$

From Equation (21), we obtain $(-c_1 - c_2\Lambda^2)\alpha - c_2\alpha^3/8 = 0$. This indicates $\alpha = 0$ due to $c_1 > 0$ and $c_2 > 0$. Therefore, the free-oscillation solution will decay with time and the first-order approximate solution will only include the composition excited by the external loads. This outcome can be confirmed by numerical simulations of Equation (11), as shown in Figure 2. While the free-oscillation term is decaying, its frequency is a function of the amplitude α .

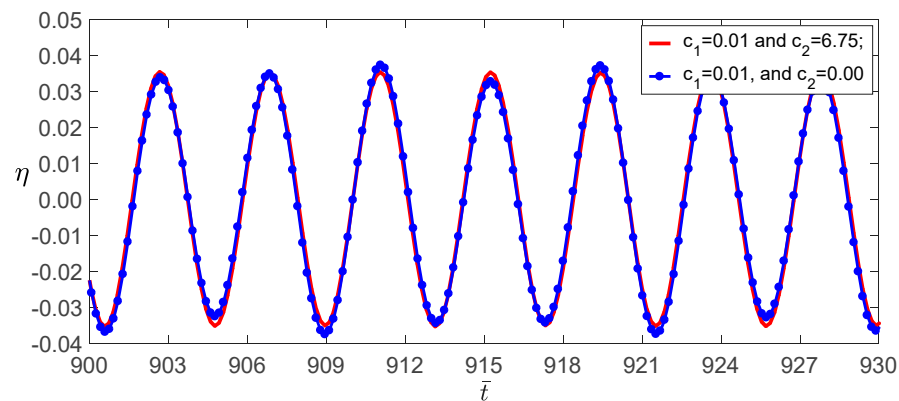


Figure 2. Time evolution of the microbeam’s midpoint displacement of the non-resonance for $\Omega_1 = 1.5$, $f_1 = 0.5$.

3.2. Primary Resonance

When the frequency of the load Ω_2 approaches the modal frequency of the microbeam ω , the beam will appear as a relatively large amplitude response. Under this condition, let $f_1 = 0$ and $\Omega_2 = \omega + \varepsilon^2\sigma$, thus the solvable condition of Equation (17) can be written as:

$$-i2\omega(A' + cA) - (ic_2\omega + 3d)A^2\bar{A} + \frac{1}{2}f_2 \exp(i\sigma T_2) = 0 \tag{23}$$

Substituting Equation (19) into Equation (23), then separating the real and imaginary parts, we obtain:

$$\alpha' = -c_1\alpha - \frac{1}{8}c_2\alpha^3 + \frac{f_2}{2\omega} \sin \gamma, \quad \alpha\gamma' = \sigma\alpha - \frac{3}{8\omega}d\alpha^3 + \frac{f_2}{2\omega} \cos \gamma \tag{24}$$

where $\gamma = \sigma T_2 - \beta$. The steady-state motions occur when $\alpha' = \gamma' = 0$, which correspond to the singular points of Equation (24). The steady-state solutions can be obtained by the following algebraic equation [26]:

$$\left[c_1^2 + \sigma^2 + \frac{1}{4} \left(c_1c_2 - \frac{3d\sigma}{\omega} \right) a^2 + \frac{1}{64} \left(c_2^2 + \frac{9d^2}{\omega^2} \right) a^4 \right] a^2 = \left(\frac{f_2}{2\omega} \right)^2 \tag{25}$$

The stability of the steady-state solutions can be judged by an investigation of the nature of the singular points of Equation (24). Letting $a = a_0 + a_1$ and $\gamma = \gamma_0 + \gamma_1$, substituting them into Equation (24), then expanding the small a_0 and γ_0 , and maintaining the linear terms in a_1 and γ_1 , we obtain:

$$\begin{aligned} \alpha'_1 &= \left(-c_1 - \frac{3}{8}c_2\alpha_0^2 \right) \alpha_1 + \frac{\gamma_1 f_2 \cos \gamma_0}{2\omega} \\ \gamma'_1 &= - \left(\frac{f \cos \gamma_{01}}{2\omega\alpha_0^2} + \frac{3d\alpha_0}{4} \right) \alpha_1 - \frac{\gamma_1 f_2 \sin \gamma_0}{2\omega\alpha_0} \end{aligned} \tag{26}$$

where a_0 and γ_0 are the singular points of Equation (24), which are used in Equation (26). The stability of the steady-state motions depends on the eigenvalues of the coefficient matrix on the right-hand side of Equation (26). If the real parts of the eigenvalues are greater than zero, the solutions are unstable [25]. Therefore, the steady-state motions are unstable when

$$\left(\frac{3c_2\alpha_0^2}{8} + c_1 \right) \left(\frac{c_2\alpha_0^2}{8} + c_1 \right) + \left(\frac{3d\alpha_0^2}{8\omega} - \sigma \right) \left(\frac{9d\alpha_0^2}{8\omega} - \sigma \right) < 0 \tag{27}$$

Equation (27) indicates that nonlinear damping affects the stability of the steady-state solutions.

4. Discussion

In this section, we use the following parameters as an example to study the effects of nonlinear damping on microbeam vibrations [16]: $E = 1.44$ GPa, $G = 0.5127$ GPa, and mass density $\rho = 1220$ kg/m³. The beam’s geometrical parameters are $L = 100$ μ m, $b = 10$ μ m, and $h = 20$ μ m, thus we have $S = 2 \times 10^2$ (μ m)², $m = \rho S = 2.44 \times 10^{-7}$ kg/m, $I = 2 \times 10^4/3$ (μ m)⁴. Let $\xi = 20$ μ m and $P_0 = 0.188$ N, thus we obtain $\omega_0 = 1.42 \times 10^7$, $\omega = 0.901$, $d = 21.3$, and $C_2 = 450C_1$. Suppose that $\bar{c}_1 = 0.01$, thus we obtain $c_1 = 6.75$.

In Section 3.1, it is theoretically demonstrated that nonlinear damping does not affect the vibration amplitudes under the non-resonant condition. Here, the numerical calculations of Equation (11) with $(f_1, \Omega_1) = (0.5, 1.5)$ confirm this prediction, as shown in Figure 2. However, when the exciting amplitude increases, for example $(f_1, \Omega_1) = (10, 1.5)$, multi-frequency vibrations will appear in the system without nonlinear damping, as shown in Figure 3. In this case, the perturbation methods are no longer applicable, since the strong excitations allow for Equation (11) to appear nonlinearly strong. When the large-amplitude vibrations of non-resonant excitations appear, nonlinear damping significantly reduces the vibration amplitudes, and suppresses the vibration components of non-excited frequencies, as shown in Figure 3.

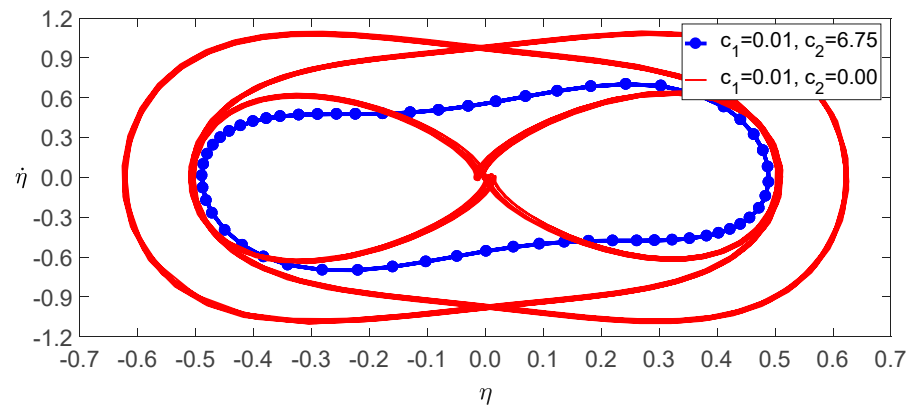


Figure 3. The phase portraits of non-resonant excitations for $\Omega_1 = 1.5$ and $f_1 = 10$.

The influence of nonlinear damping on primary resonance is mainly shown in the following two aspects: First, when the exciting frequency is greater than the modal frequency of the microbeam, nonlinear damping can significantly change the bifurcation points of the load and strongly affects the dynamic behavior of the microbeam, as shown in Figures 4 and 5. Second, when the exciting frequency is less than the modal frequency of the microbeam, the impact of nonlinear damping is slight, as shown in Figures 5 and 6. The numerical calculations of Equation (11) confirm the aforementioned results, as shown in Figures 7 and 8. For example, when $f_2 = 3$ and $\sigma = 10$, the vibration amplitude with $c_2 = 0$ is about six times larger than the amplitude with $c_2 = 6.75$, as shown in Figure 7. This difference is essential in practice.

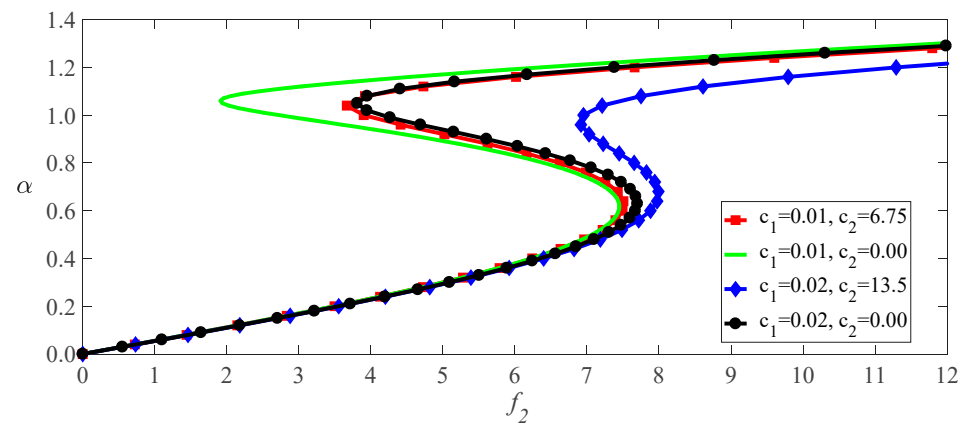


Figure 4. Amplitude of the response as a function of the excitation amplitude of primary resonance with $\sigma = 10$ for several damping parameters.

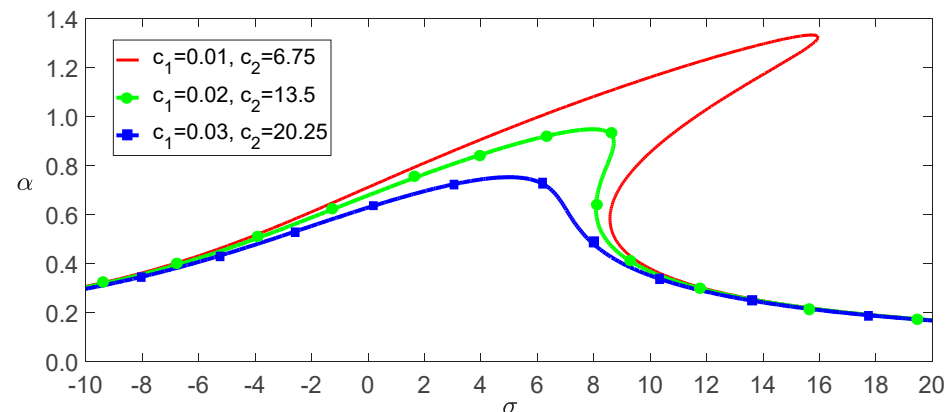


Figure 5. Frequency-response curves of primary resonance for $f_2 = 6$.

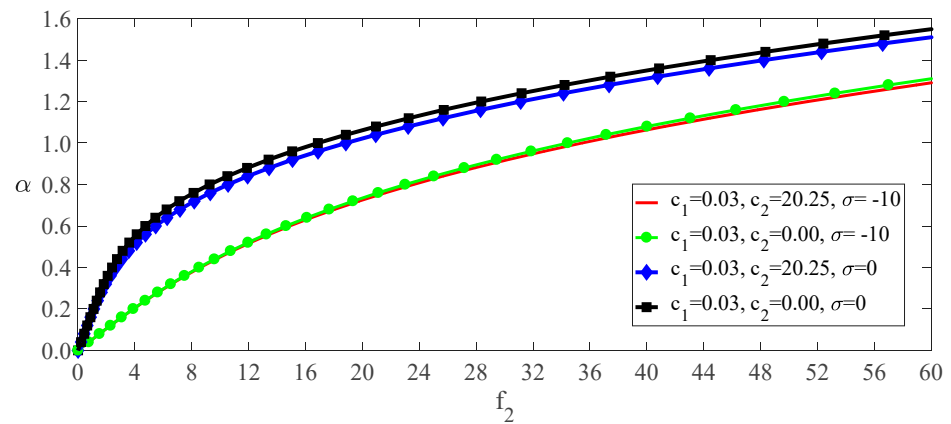


Figure 6. Amplitude of the response as a function of the excitation amplitude of primary resonance with $\sigma = -10$ for several damping parameters.

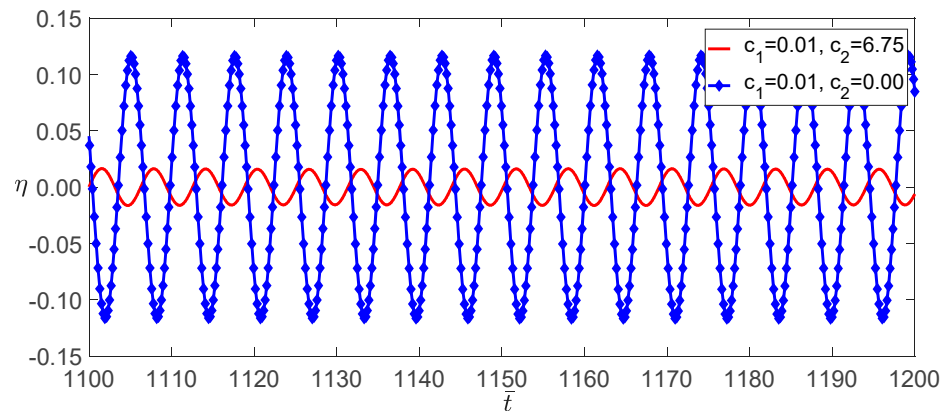


Figure 7. Time evolution of the microbeam's midpoint displacement of primary resonance for $f_2 = 3$ and $\sigma = 10$.

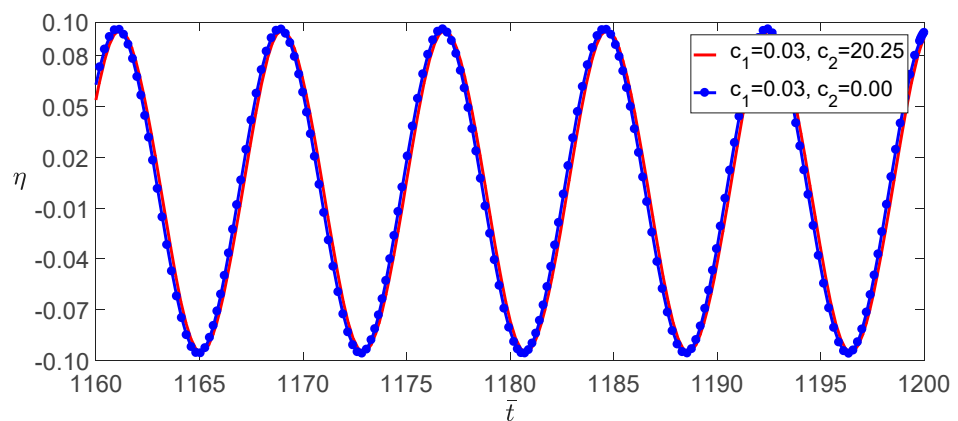


Figure 8. Time evolution of the microbeam's midpoint displacement of primary resonance for $f_2 = 30$ and $\sigma = -10$.

Nonlinear elastic effects play an essential role in the dynamics of MEMS [1,2]. Nonlinear dissipation effects in micromechanical oscillators are often overlooked. However, our work shows that arbitrarily overlooking nonlinear damping may lead to qualitative mistakes. In this paper, we especially focus on the system's behavior near the bifurcation points of primary resonance. The results show that nonlinear damping has a significant impact on the dynamics of microbeams, as shown in Figures 4 and 6. Moreover, it is necessary to research particular vibrations, such as the super-resonance and sub-resonance. Furthermore, the experimental results suggest that linear Kelvin–Voigt damping cannot

fully account for all of the experimentally observed nonlinear dissipation [22]. We believe that the effects of nonlinear damping in microbeams necessitate further studies, both experimentally and theoretically.

5. Conclusions

In the present paper, we propose a new partial differential equation to represent nonlinear oscillations of the microbeam. The new model considers the small-scale effect and nonlinear terms, which are induced by the axial elongation of the beam and Kelvin–Voigt damping. Here, we solved the model using the Galerkin and multiple scale methods. The results show that nonlinear damping affects the microbeam vibrations in the following three aspects: First, under the non-resonant condition, nonlinear damping scarcely affects the small-amplitude vibrations. However, in the large-amplitude vibrations, nonlinear damping remarkably reduces the amplitudes and suppresses the multi-period vibrations. Second, nonlinear damping slightly decreases the vibration amplitudes when the frequency of the load is less than the modal frequency of the microbeam under the primary resonance condition. Third, when the frequency of the load is greater than the modal frequency under the primary resonance condition, nonlinear damping can significantly change the bifurcation points of the load and strongly affects the vibrations. The present research suggests that the accurate description of microbeam vibrations must consider nonlinear damping.

Author Contributions: Conceptualization, K.H. and W.X.; methodology, K.H. and T.L.; software, T.L. and L.C.; validation, K.H. and L.C.; formal analysis, K.H.; investigation, K.H.; resources, K.H.; writing—original draft preparation, K.H.; writing—review and editing, K.H.; project administration, K.H.; funding acquisition, K.H. All authors have read and agreed to the published version of the manuscript.

Funding: This research was funded by the National Natural Science Foundation of China (grant numbers 11562009 and 12050001).

Institutional Review Board Statement: Not applicable.

Informed Consent Statement: Not applicable.

Data Availability Statement: The data presented in this study are available in the article insert.

Conflicts of Interest: The authors declare no conflict of interest.

References

1. Lee, K.B. *Principles of Microelectromechanical Systems*; John Wiley & Sons: New York, NY, USA, 2011.
2. Maluf, N.; Williams, K. *An Introduction to Microelectromechanical Systems Engineering*; Artech House: Boston, MA, USA, 2004.
3. Huang, K.; Qu, B.; Li, Z.; Yao, J. Nonlinear microstructure-dependent Bernoulli–Euler beam model based on the modified couple stress theory and finite rotation of section. *Micro Nano Lett.* **2018**, *13*, 490–493. [[CrossRef](#)]
4. McFarland, A.W.; Colton, J.S. Role of material microstructure in plate stiffness with relevance to microcantilever sensors. *J. Micromech. Microeng.* **2005**, *15*, 1060–1067. [[CrossRef](#)]
5. Fleck, N.A.; Muller, G.M.; Ashby, M.F.; Hutchinson, J.W. Strain gradient plasticity: Theory and experiment. *Acta Metall. Mater.* **1994**, *42*, 475–487. [[CrossRef](#)]
6. Stölken, J.S.; Evans, A.G. A microbend test method for measuring the plasticity length scale. *Acta Mater.* **1998**, *46*, 5109–5115. [[CrossRef](#)]
7. Reddy, J.N. Nonlocal theories for bending, buckling and vibration of beams. *Int. J. Eng. Sci.* **2007**, *45*, 288–307. [[CrossRef](#)]
8. Huang, K.; Zhang, S.; Li, J.; Li, Z. Nonlocal nonlinear model of Bernoulli–Euler nanobeam with small initial curvature and its application to single-walled carbon nanotubes. *Microsyst. Technol.* **2019**, *25*, 4303–4310. [[CrossRef](#)]
9. Reddy, J.N.; Ruocco, E.; Loya, J.A.; Neves, A.M.A. Theories and Analysis of Functionally Graded Beams. *Appl. Sci.* **2021**, *11*, 7159. [[CrossRef](#)]
10. D’Annibale, F.; Ferretti, M.; Luongo, A. Static and dynamic responses of micro-structured beams. *Appl. Sci.* **2020**, *10*, 6836. [[CrossRef](#)]
11. Kahrobaian, M.H.; Asghari, M.; Rahaeifard, M.; Ahmadian, M. A nonlinear strain gradient beam formulation. *Int. J. Eng. Sci.* **2011**, *49*, 1256–1267. [[CrossRef](#)]
12. Huang, K.; Cai, X.; Wang, M. Bernoulli–Euler beam theory of single-walled carbon nanotubes based on nonlinear stress-strain relationship. *Mater. Res. Express* **2020**, *7*, 125003. [[CrossRef](#)]

13. Yang, F.; Chong, A.C.M.; Lam, D.C.C.; Tong, P. Couple stress based strain gradient theory for elasticity. *Int. J. Solids Struct.* **2002**, *39*, 2731–2743. [[CrossRef](#)]
14. Park, S.K.; Gao, X.L. Bernoulli–Euler beam model based on a modified couple stress theory. *J. Micromech. Microeng.* **2006**, *16*, 2355. [[CrossRef](#)]
15. Ma, H.M.; Gao, X.L.; Reddy, J.N. A microstructure-dependent Timoshenko beam model based on a modified couple stress theory. *J. Mech. Phys. Solids* **2008**, *56*, 3379–3391. [[CrossRef](#)]
16. Xia, W.; Wang, L.; Yin, L. Nonlinear non-classical microscale beams: Static bending, postbuckling and free vibration. *Int. J. Eng. Sci.* **2010**, *48*, 2044–2053. [[CrossRef](#)]
17. Farokhi, H.; Ghayesh, M.H.; Hussain, S. Large-amplitude dynamical behaviour of microcantilevers. *Int. J. Eng. Sci.* **2016**, *106*, 29–41. [[CrossRef](#)]
18. Noori, H.R.; Jomehzadeh, E.A. Levy-type solution for buckling analysis of micro-plates considering the small length scale. *Mech. Ind.* **2014**, *15*, 225–232. [[CrossRef](#)]
19. Ke, L.L.; Wang, Y.S.; Yang, J.; Kitipornchai, S. Free vibration of size-dependent Mindlin microplates based on the modified couple stress theory. *J. Sound. Vib.* **2012**, *331*, 94–106. [[CrossRef](#)]
20. Dehrouyeh-Semnani, A.M.; Nikkhah-Bahrami, M.; Yazdi, M.R.H. On nonlinear vibrations of micropipes conveying fluid. *Int. J. Eng. Sci.* **2017**, *117*, 20–33. [[CrossRef](#)]
21. With, G.D. *Structure, Deformation, and Integrity of Materials: Volume 1: Fundamentals and Elasticity*; Wiley-VCH: Weinheim, Germany, 2006.
22. Zaitsev, S.; Shtempluck, O.; Buks, E.; Gottlieb, O. Nonlinear damping in a micromechanical oscillator. *Nonlinear Dyn.* **2012**, *67*, 859–883. [[CrossRef](#)]
23. Park, S.K.; Gao, X.L. Variational formulation of a modified couple stress theory and its application to a simple shear problem. *Z. Angew. Math. Phys.* **2008**, *59*, 904–917. [[CrossRef](#)]
24. Hertzberg, R.W.; Vinci, R.P.; Hertzberg, J.L. *Deformation and Fracture Mechanics of Engineering Materials*; John Wiley & Sons: New York, NY, USA, 2020.
25. Nayfeh, A.H.; Pai, P.F. *Linear and Nonlinear Structural Mechanics*; John Wiley & Sons: New York, NY, USA, 2008.
26. Washizu, K. *Variational Methods in Elasticity and Plasticity*; Pergamon Press: Oxford, UK, 1968.
27. Nayfeh, A.H.; Mook, D.T. *Nonlinear Oscillations*; John Wiley & Sons: New York, NY, USA, 1980.
28. Huang, K.; Feng, Q.; Qu, B. Bending aeroelastic instability of the structure of suspended cable-stayed beam. *Nonlinear Dyn.* **2017**, *87*, 2765–2778. [[CrossRef](#)]
29. Luongo, A.; Paolone, A. On the reconstitution problem in the multiple time-scale method. *Nonlinear. Dyn.* **1999**, *19*, 135–158. [[CrossRef](#)]
30. Huang, K.; Yao, J. Beam Theory of Thermal-Electro-Mechanical Coupling for Single-Wall Carbon Nanotubes. *Nanomaterials* **2021**, *11*, 923. [[CrossRef](#)] [[PubMed](#)]